

Results from the Spin Program at COSY-ANKE

A. KACHARAVA¹ AND C. WILKIN²

¹*Institut für Kernphysik and Jülich Centre for Hadron Physics,
Forschungszentrum Jülich, D-52425 Jülich, Germany*

²*Physics and Astronomy Department, UCL, Gower Street, London WC1E 6BT, U.K.*

QUERY SHEET

This page lists questions we have about your paper. The numbers displayed at the left can be found in the text of the paper for reference. You will find these queries displayed as small gray boxes within the text or in the margin areas.

In addition, please review your paper as a whole for correctness, paying close attention to special characters and math symbols.

<AQ1>update for reference 16?</AQ>

Results from the Spin Program at COSY-ANKE

A. KACHARAVA¹ AND C. WILKIN²

¹*Institut für Kernphysik and Jülich Centre for Hadron Physics,
Forschungszentrum Jülich, D-52425 Jülich, Germany*

²*Physics and Astronomy Department, UCL, Gower Street, London WC1E 6BT, U.K.*

Introduction

It was once claimed that in strong interaction physics “Spin is an inessential complication” [1]. This rather negative attitude ignores certain practical applications and surely dismisses the beauty inherent in many phenomena involving particle polarization. Recognizing this, a program was outlined several years ago to exploit the possibilities of carrying out experiments with polarized beams and targets at ANKE [2]. This facility is based around a magnetic spectrometer sited at an internal target station of the COoler SYNchrotron and storage ring COSY of the Forschungszentrum Jülich. The basic features of the complex were described in a previous issue [3] and we shall here concentrate on a few of the fruits of the spin program.

COSY can accelerate and store polarized protons and vector and tensor polarized deuterons up to momenta of 3.7 GeV/c. In addition to unpolarized hydrogen and deuterium cluster-jet targets, ANKE is also equipped with polarized \vec{H} and \vec{D} gas target cells so that spin correlations can be studied as well as beam and target analyzing powers.

In the following three sections we first show how, in experiments with polarized deuteron beams at a storage ring, the beam momentum can be determined very precisely through the study of artificially induced depolarizing resonances. This led to a determination of the mass of the η meson that is as precise as any other in the literature. The nucleon–nucleon program has two distinct elements, the most developed being the charge exchange of tensor polarized deuterons, which gives immediate access to the tensor amplitudes in large angle neutron–proton scattering. However, in addition, measurements are made in proton–proton elastic scattering with a polarized beam in angular regions where little reliable data exist. Finally, a variety of spin-dependent data on pion production in nucleon–nucleon collisions near threshold have been taken and analyzed. These permitted a full partial-wave analysis to be carried out in the domain where two protons emerge almost bound.

Beam Momentum Determination and the Mass of the η Meson

A big challenge that one often faces in a precision experiment at a storage ring is the determination of the beam momentum with sufficient accuracy. Although the revolution frequency f_0 can be measured with a relative precision of around 10^{-5} , there are much greater uncertainties in the exact orbit of the particles in the ring. A way of overcoming this problem was proposed many years ago [4] and has since been implemented at several electron colliders. Spin is here very much the *essential* element.

The spin of a polarized beam particle in a storage ring precesses around the normal to the plane of the machine. A horizontal *rf* field from a solenoid can induce depolarizing resonances such that the beam depolarizes when the frequency of the externally applied field coincides with that of the spin precession in the ring. The depolarizing resonance frequency f_r depends on the revolution frequency of the machine and the kinematical factor $\gamma = E/mc^2$, where E and m are, respectively, the total energy and mass of the particle. For a planar accelerator where there are no horizontal fields,

$$f_r/f_0 = k + \gamma G, \quad (1)$$

where G is the particle’s gyromagnetic anomaly and k is an integer. The combination of the measurements of the revolution and depolarizing frequencies allows the evaluation of γ and hence the beam momentum p .

The depolarizing resonance technique was applied for the first time at COSY with a vector polarized deuteron beam of momenta around 3.1 GeV/c [5]. The deuterons were accelerated with an *rf* cavity and, once the required momentum was reached, a barrier bucket cavity was used to compensate for the energy losses incurred through the beam-target interactions. The depolarizing solenoid had an integrated maximum longitudinal *rf* magnetic field of $\int B_{\text{rms}} d\ell = 0.67$ Tmm at an *rf* voltage of 5.7 kV rms. The value of $k = 1$ in Equation (1) corresponds to frequencies that were in the middle of the solenoid range of 0.5–1.5 MHz.

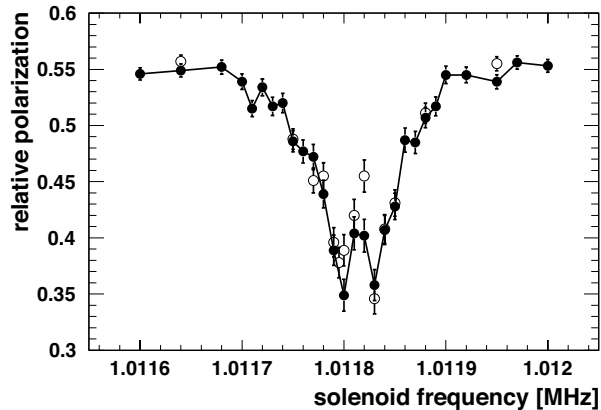


Figure 1. Spin-resonance measurements at a single beam momentum (closed circles). The open symbols represent results obtained for an extended cycle time, where the perturbing solenoid was switched on after 178 s.

A vector polarized deuteron beam leads to an asymmetry in the scattering from a carbon target, which could be measured with the EDDA detector [6]. Since only the frequency of the depolarizing resonance needed to be determined, an absolute calibration of this device at different deuteron momenta was not required. Figure 1 displays an example of this relative polarization as a function of the solenoid frequency for a fixed beam momentum. When the frequency of the solenoid coincides with the spin-precession frequency, the beam is maximally depolarized. The structures, especially the double peak in the center, are caused by the interaction of the deuteron beam with the barrier bucket cavity. However, these did not affect the mean position, which could be fixed with a precision of $\approx 10^{-5}$. The full width at half

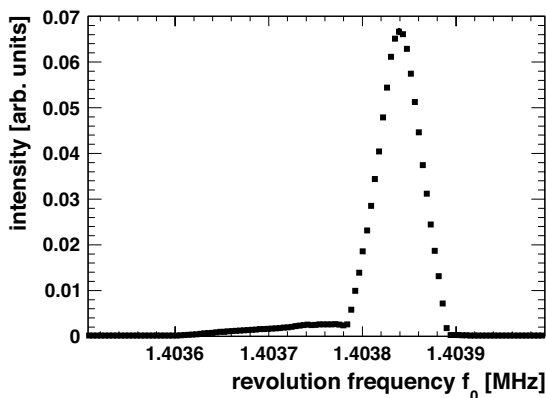


Figure 2. Mean Schottky power spectrum at one beam momentum. The statistical error bars lie within the data points.

maximum, which was typically in the region of 80–100 Hz, is mainly a reflection of the momentum spread within the beam. If this were the only significant effect, it would correspond to $\delta p/p_{\text{rms}} \approx 2 \times 10^{-4}$.

The other frequency required in the evaluation of Eq. (1) (i.e., that of the circulation in COSY), was measured by using the Schottky noise of the deuteron beam. The statistical distribution of the charged particles in the beam leads to random current fluctuations that induce a voltage signal at a beam pick-up in the ring. The Fourier transform of this voltage-to-time signal by a spectrum analyser delivers the frequency distribution around the harmonics of the revolution frequency of the beam. As mentioned later this phenomenon is also used at COSY to measure the luminosity in an experiment [7]. All the data acquired at a particular beam momentum are presented in Figure 2. The small tail seen at low frequencies corresponds to beam particles that escaped the influence of the barrier bucket cavity but still circulated in COSY. The statistical uncertainty in the weighted arithmetic mean was in all cases below 0.2 Hz compared to the typical 1.4 MHz shown in the figure. This means that, under ideal conditions, the left hand side of Eq. (1) could be measured with a precision of better than 10^{-5} .

The great efforts expended in determining precisely the deuteron beam momentum were justified in order to measure the mass of the h meson from the missing-mass peak in the $dp \rightarrow {}^3\text{He } X$ reaction [8]. For this purpose the experiment was carried out at twelve closely spaced deuteron momenta a little above the η threshold and two just below to provide the information required to subtract the multipion background. By exploiting its full geometric acceptance near threshold, it was possible to calibrate the ANKE spectrometer very precisely and thus determine the final ${}^3\text{He}$ CM momentum p_f for each of the twelve deuteron beam momenta and the results are shown in Figure 3. Although the method depends primarily upon the determination of the kinematics rather than counting rates, its implementation is helped enormously by the fact that the cross-section jumps to its plateau value already by the first point in Figure 3 [9].

The long lever arm facilitates a robust extrapolation to the η threshold, where the deuteron momentum was found to be $p_d = 3141.686 \pm 0.021$ MeV/c. There is a one-to-one relation between this and the mass of the meson, which is found to be

$$m_\eta = (547.873 \pm 0.005_{\text{stat}} \pm 0.026_{\text{sys}}) \text{ MeV}/c^2.$$

It is in fact the determination of the threshold beam momentum that provides the largest contribution to the 26 keV/c²

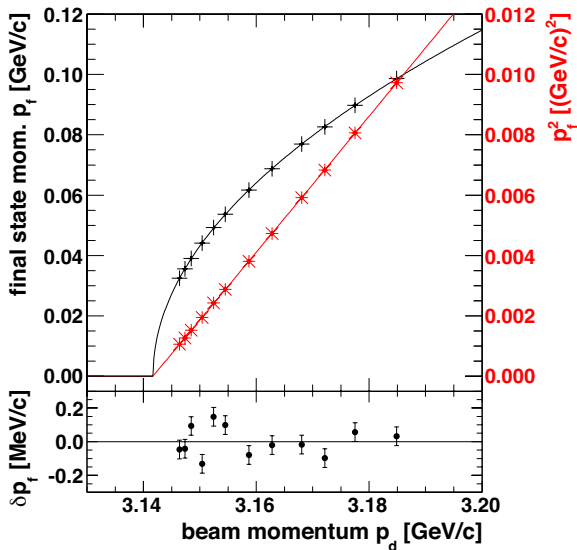


Figure 3. Values of the final-state CM momentum p_f (black crosses) and its square (red stars) plotted against the deuteron laboratory momentum p_d . The lower panel shows the deviations of the experimental data from the fitted curve in p_f .

systematic uncertainty. The result is compatible with all the modern measurements reported by the Particle Data Group [10] that studied the η decay and the error bars are as small as any of these. The result suggests that earlier missing-mass determinations, which differed by ~ 0.5 keV/ c^2 , lacked the necessary precision.

The Nucleon–Nucleon Program

A good understanding of the nucleon–nucleon (NN) interaction still remains one of the principal goals of nuclear and hadronic physics. Apart from their intrinsic importance for the study of nuclear forces, NN elastic scattering data are also necessary ingredients in the modelling of meson production and other nuclear reactions at intermediate energies. It therefore goes without saying that all facilities should try to fill in the remaining gaps in our knowledge in the area.

The COSY–EDDA collaboration [6] produced a wealth of data on proton–proton elastic scattering that completely revolutionised the isospin $I = 1$ NN phase-shift analysis up to about 2.1 GeV [11]. However, for proton energies above 1 GeV, very little is known about the pp elastic differential cross-section or analyzing power for center-of-mass angles $10^\circ < \theta_{\text{cm}} < 30^\circ$. The cross-section data that do exist seem to fall systematically below the predictions of the SAID partial-wave analysis [11]. In this angular range the

fast proton emerging at small angles from a hydrogen target can be measured well in the ANKE magnetic spectrometer, whereas the slow recoil proton emerging at large angles can be measured independently in one of the Silicon Tracking Telescopes. The luminosity that is so crucial for the determination of the absolute cross-sections can be determined using the Schottky method [7] that was mentioned in the previous section. Preliminary data are already available on the differential cross-sections at eight energies and approval has been given to measure the proton analyzing powers at the same energies.

Much greater effort has been made in the study of the spin-dependent terms in large angle neutron–proton scattering. It was pointed out many years ago that the $dp \rightarrow \{pp\}_s n$ charge exchange at small angles is very sensitive to the spin-spin terms in the $np \rightarrow pn$ amplitude pro-

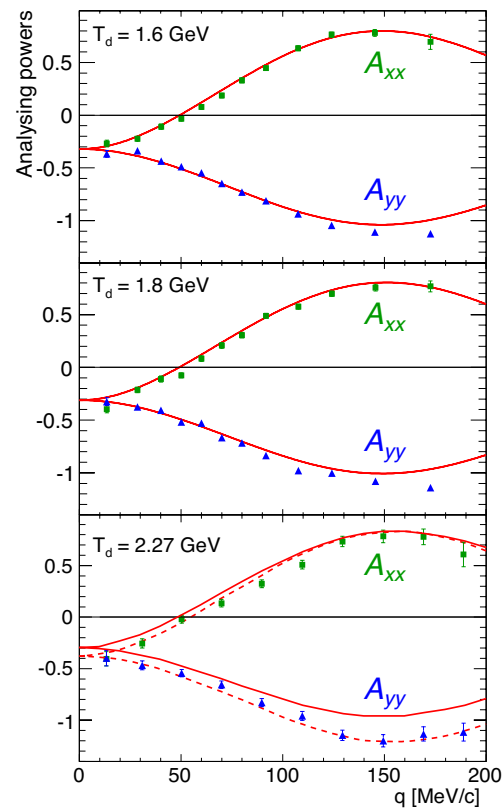


Figure 4. Cartesian deuteron analyzing powers for the $\vec{d} \rightarrow \{pp\}_s n$ reaction for $E_{pp} < 3$ MeV at $T_d = 1.6, 1.8,$ and 2.27 GeV [16]. The impulse approximation predictions [17] have been evaluated with the SAID amplitudes [11] (solid curves) and also, at the highest energy, when the longitudinal spin-spin amplitude is scaled by a factor of 0.75 (dashed curves).

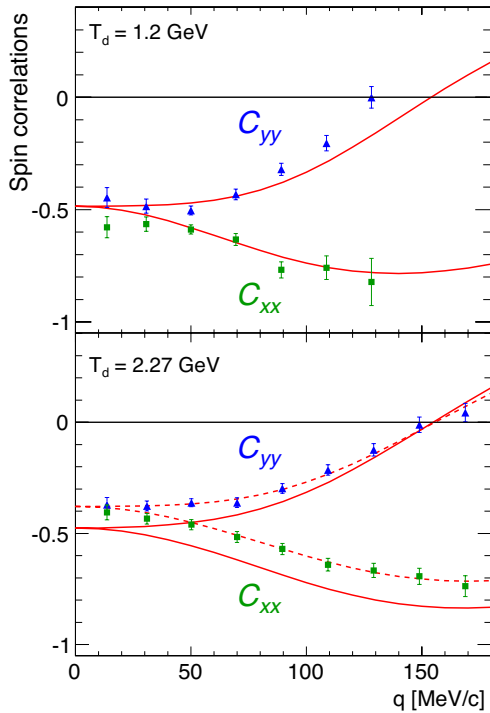


Figure 5. Transverse spin correlation parameters in the $\vec{d}\vec{p} \rightarrow \{pp\}_s n$ reaction at (a) 1.2 and (b) 2.27 GeV [16] compared to the predictions of an impulse approximation model (solid curves). Better agreement is found at the higher energy if the longitudinal input is scaled by a factor of 0.75 (dashed curves).

vided the excitation energy E_{pp} in the final pp system is kept low [12]. Under such conditions the $\{pp\}_s$ is in a 1S_0 state and the charge exchange necessarily involves a spin flip from the initial np spin-triplet of the deuteron. Furthermore, measurements of the deuteron tensor analyzing powers A_{xx} and A_{yy} allow one to distinguish between the contributions from the three spin-spin np amplitudes.

Measurements were carried out at Saclay [13, 14], but only in regions where the NN amplitudes were reasonably well known. These have been extended in fine steps in momentum transfer q to higher energy at ANKE [15, 16]. A cut of $E_{pp} < 3$ MeV was typically imposed but any contamination from spin-triplet P -waves was taken into account in the theoretical modelling [17]. The ANKE analyzing power results at 1.6, 1.8, and 2.27 GeV are compared in Figure 4 to these impulse approximation predictions using up-to-date np amplitudes [11] as input. The satisfactory agreement at the two lower energies, and also in the values of the differential cross-sections, shows that the theoretical description is adequate here.

Above about 1 GeV neutron–proton data are rather sparse. It comes therefore as no surprise that, when the same approach is employed for the highest energy data shown in Figure 4, the current SAID amplitudes [11] give a poor overall description of the results. However, if the longitudinal spin-spin amplitude is multiplied by a global factor of 0.75, the agreement is much more satisfactory. This is clear evidence that the charge exchange data can provide useful input to the NN database.

Confirmation of these conclusions is to be found in the studies of the deuteron–proton spin correlation parameters measured with the polarized hydrogen gas cell. Results on this are shown in Figure 5. In impulse approximation, these observables are sensitive to the interference between the longitudinal spin-spin amplitude and the two transverse ones. Whereas there is satisfactory agreement with the theoretical predictions at 1.2 GeV, the model is much more satisfactory at 2.27 GeV if the longitudinal input is scaled by a factor of 0.75.

In addition to measuring the spin correlations with the polarized cell, data were also obtained on the proton analyzing power in the $\vec{d}\vec{p} \rightarrow \{pp\}_s n$ reaction and the results are shown in Figure 6. The message here is very similar to that for the other observables. At 600 MeV per nucleon the SAID input reproduces the experimental points very well but it seems that at 1135 MeV the SAID description of the spin-orbit amplitude has serious deficiencies.

As well as studying the $\vec{d}\vec{p} \rightarrow \{pp\}_s X$ data to extract the neutron as a missing-mass peak, results were also obtained where $m_x > m_n + m_\pi$. These events must be associated with pion production, especially through the Δ isobar. The

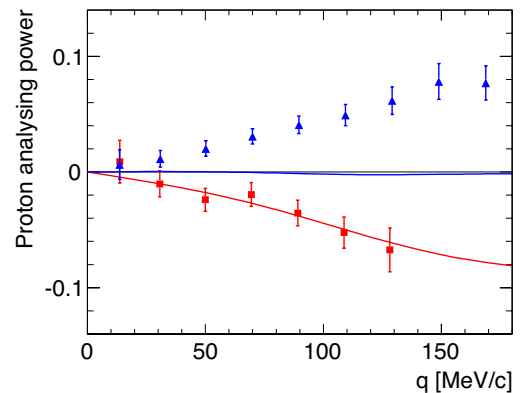


Figure 6. Proton analyzing power in the $\vec{d}\vec{p} \rightarrow \{pp\}_s n$ reaction at 1.2 GeV (red squares) and 2.27 GeV (blue triangles) [16] compared to impulse approximation predictions. Note that, with the current SAID input [11], the latter almost vanish at the higher energy.

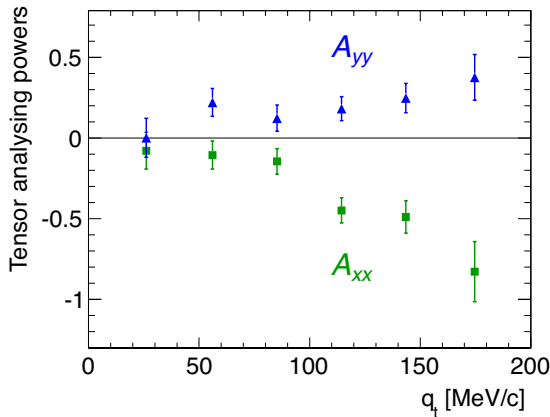


Figure 7. Tensor analyzing powers for the $\vec{d}p \rightarrow \{pp\}_s X$ reaction at 2.27 GeV as a function of the transverse momentum transfer. The data are integrated over the mass range $1.19 < M_X < 1.35 \text{ GeV}/c^2$ [18].

first indications shown in Figure 7 are that the Cartesian analyzing powers are largely opposite in sign to those for $\vec{d}p \rightarrow \{pp\}_s n$ [18]. These data should yield information on the amplitude structure of the $NN \rightarrow N\Delta$ reaction.

Pion Production in Nucleon–Nucleon Collisions

One of the priorities at ANKE is to perform a complete set of measurements of $NN \rightarrow \{pp\}_s \pi$ at low energy. Since, as mentioned earlier, the $\{pp\}_s$ proton–proton pair is overwhelmingly in the 1S_0 state, only the polarizations of the initial nucleons have to be studied. As parts of this program, the differential cross-section and analyzing power of the $\vec{p}p \rightarrow \{pp\}_s \pi^0$ reaction were measured at 353 MeV [19] and the same observables measured in quasi-free π^- production on the deuteron, $\vec{p}d \rightarrow p_{\text{sp}} \{pp\}_s \pi^-$ [20], where p_{sp} is a “spectator” proton. By making certain theoretical assumptions and retaining amplitudes up to pion d -waves, the combined data sets are sufficient for a partial-wave decomposition. This is of particular interest for Chiral Perturbation Theory, where it is important to establish that the same short-range $NN \rightarrow NN\pi$ vertex that contributes to p -wave pion production is consistent with other intermediate energy phenomena.

For π^0 production, both protons were measured in the ANKE Forward Detector. After selecting the 1S_0 final state, the kinematics of the $\vec{p}p \rightarrow \{pp\}_s X$ process could be reconstructed on an event-by-event basis to obtain the π^0 rate from the missing-mass M_X spectrum. By using a beam with a $\pm 68\%$ polarization, the cross-section and analyzing power could be measured simultaneously and the results are shown in Figures 8 and 9.

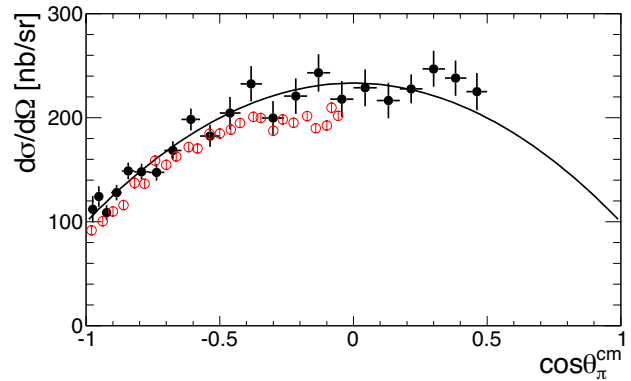


Figure 8. Differential cross-section for the $pp \rightarrow \{pp\}_s \pi^0$ reaction at 353 MeV. The ANKE measurements (solid black) circles are compared with the CELSIUS data (open red) circles at 360 MeV [21]. The curve is the partial-wave fit.

The cross-section data agree quite well over most of the angular range with those taken at CELSIUS [21] and the strong anisotropy is evidence for significant d -wave pion production. In the absence of pion d - (or higher) waves the

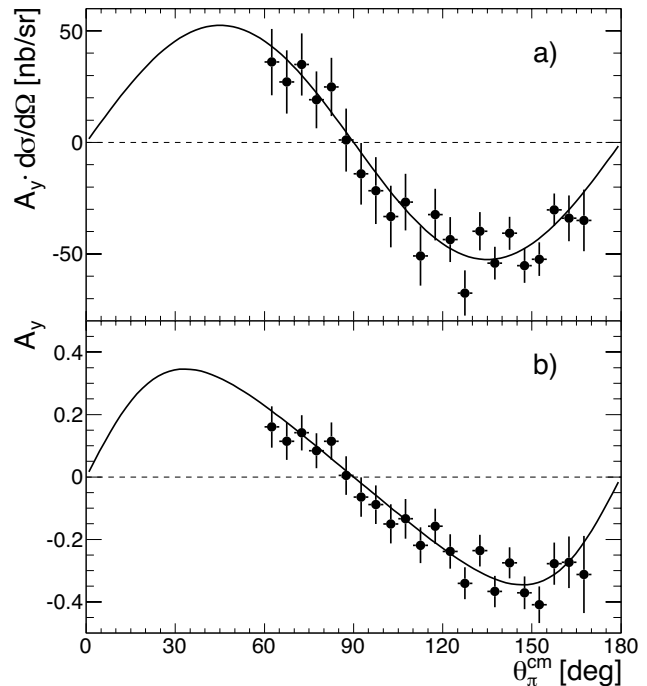


Figure 9. (a) Product of the measured analyzing power and differential cross-section for the $\vec{p}p \rightarrow \{pp\}_s \pi^0$ reaction. (b) Measured values of A_y ; the overall systematic uncertainty is $\approx 5\%$. The curves are partial-wave fits.

analyzing power would vanish and, as seen in Figure 9, this is far from being the case.

In the $\vec{p}d \rightarrow p_{\text{sp}}\{pp\}_s\pi^-$ experiment, three particles had to be detected in the final state to identify the reaction. In addition to the two protons in the 1S_0 state, either the π^- or the third (slow) proton must be measured, the latter in one of the silicon tracking telescopes placed in the target chamber. Together the two detection modes led to a full angular coverage. In either case the slow proton was restricted kinematically to be a spectator so that the cross-section and analyzing power of the quasi-free $\vec{p}n \rightarrow \{pp\}_s\pi^-$ reaction could be extracted in the 353 ± 20 MeV interval, the results being shown in Figures 10 and 11.

The differential cross-section agrees with the earlier TRIUMF measurement [22], except for their two most forward points. The disagreement persists with the analyzing power data measured in the forward hemisphere [23] shown in Figure 11. On the other hand, the agreement with the shape of the cross-section deduced from the $\pi^-^3\text{He} \rightarrow pnn$ reaction [24] is even better.

Even if one considers only s , p , and d -wave pion production, the cross-section and analyzing power data are insufficient to perform a full amplitude analysis without further assumptions. These were to neglect the coupling between the initial 3P_2 and 3F_2 waves and to use the Watson theo-

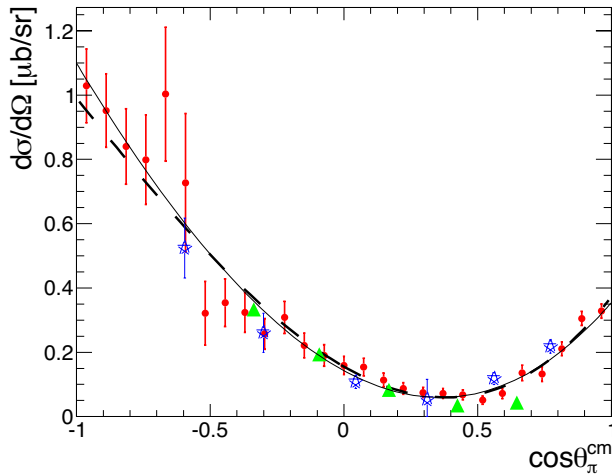


Figure 10. Differential cross-section for $pn \rightarrow \{pp\}_s\pi^-$ at $T \approx 353$ MeV. ANKE data with statistical errors are shown by red circles; the systematic error is $\approx 6\%$. The statistical errors of the TRIUMF data [22] (green triangles) are smaller than the symbols and the normalization uncertainty is 10%. The blue stars are arbitrarily scaled cross-sections extracted from pion absorption data [24]. The solid curve is a partial-wave fit to the ANKE data.

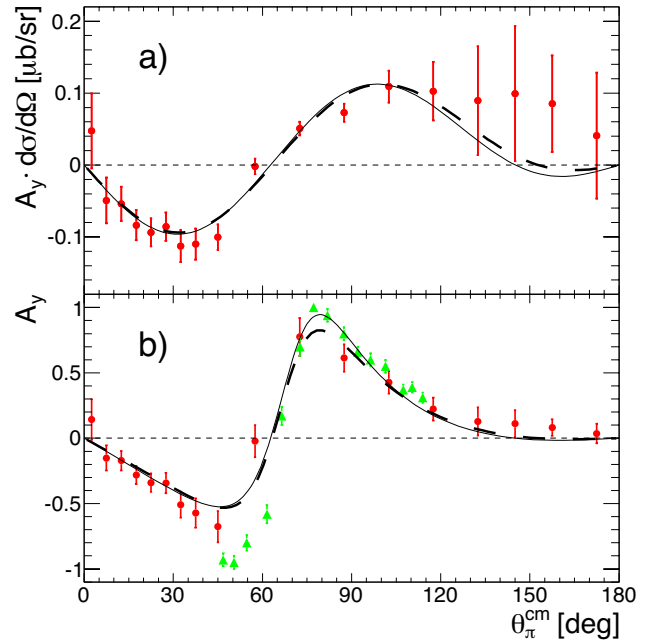


Figure 11. (a) Product of the measured analyzing power and differential cross-section for the $\vec{p}n \rightarrow \{pp\}_s\pi^-$ reaction at 353 MeV; the statistical error do not include the 11% systematic uncertainty. (b) Values of A_y measured at ANKE (circles) and TRIUMF [23] (triangles). The curves are partial-wave fits to the ANKE data.

rem to determine the phases of the production amplitudes from these and also the 3P_0 wave. There are then seven real parameters available to describe essentially ten features in Figures 8–11. The success achieved here suggests that the phase assumptions are basically correct. The analysis shows that d -wave production is confined almost purely to the 3P_2 channel but by far the largest term is associated with p -wave production from the initial 3D_1 state.

The Future

Although the partial-wave description of the pion production data is both plausible and impressive, one needs to measure other types of observables in order to test its validity. By using a polarized hydrogen gas cell in conjunction with a polarized deuteron beam, it was possible to study the transverse spin-spin correlation in the $\vec{p}n \rightarrow \{pp\}_s\pi^-$ reaction. The preliminary results are consistent with the predictions of the amplitude analysis discussed earlier. Further checks could be made through measurements of the longitudinal-transverse spin correlation but these will require the delivery, installation, and commissioning of a Siberian snake to rotate the proton spin. This should take place early

in 2013. The snake will also allow us to study the spin-correlation parameter A_{00kn} in small angle pp elastic scattering.

Although the charge exchange program with a polarized deuteron beam has been very successful, this only allows measurements to be carried out up to 1.15 GeV per nucleon. To go higher at COSY we must work in inverse kinematics and use the polarized deuterium target in conjunction with a proton beam. The charge exchange can then be studied purely through the measurement of two slow protons in the silicon tracking telescopes without using the ANKE magnetic spectrometer at all. However, this opens even more fascinating possibilities, such as the study of Δ isobar production in $\vec{p}\vec{d} \rightarrow \{pp\}_s \Delta^0$ where the spin alignment of the Δ isobar can be determined through the measurement of one of the products of the $\Delta \rightarrow p\pi^-$ decay. On the other hand, with its array of detectors, ANKE can investigate simultaneously a wide range of nuclear reactions, which makes the spin program at the facility so exciting.

References

1. G. F. Chew, *The Analytic S-matrix* (W. A. Benjamin, New York, 1966).
2. A. Kacharava, F. Rathmann, and C. Wilkin, *Spin Physics from COSY to FAIR*, COSY proposal 152 (2005), arXiv:nucl-ex/0511028.
3. M. Büscher, A. Lehrach, and F. Goldenbaum, *Nucl. Phys. News* 21 (2011) 5.
4. S. I. Serednyakov et al., *Zh. Eksp. Teor. Fiz.* 71 (1976) 2025; Ya. S. Derbenev et al., *Part. Accel.* 10 (1980) 77.
5. P. Goslawski et al., *Phys. Rev. ST Accel. Beams* 13 (2010) 022803.
6. M. Altmeier et al., *Eur. Phys. J. A* 23 (2005) 351.
7. H. J. Stein et al., *Phys. Rev. ST Accel. Beams* 11 (2008) 052801.
8. P. Goslawski et al., *Phys. Rev. D* 85 (2012) 112011.
9. T. Mersmann et al., *Phys. Rev. Lett.* 98 (2007) 242301.
10. J. Beringer et al. (Particle Data Group), *Phys. Rev. D* 86 (2012) 010001.
11. SAID data base, <http://gwdac.phys.gwu.edu>.
12. D. V. Bugg and C. Wilkin, *Nucl. Phys. A* 467 (1987) 575.
13. C. Ellegaard et al., *Phys. Rev. Lett.* 59 (1987) 974.
14. S. Kox et al., *Nucl. Phys. A* 556 (1993) 621.
15. D. Chiladze et al., *Eur. Phys. J. A* 40 (2009) 23.
16. D. Mchedlishvili et al., submitted to *Eur. Phys. J. A*, arXiv:1212.2365 [nucl-ex]. **AQ1**
17. J. Carbonell, M. B. Barbaro, and C. Wilkin, *Nucl. Phys. A* 529 (1991) 653.
18. D. Mchedlishvili, *PoS (STORI'11)*, 040 (2011), <http://pos.sissa.it>
19. D. Tsirkov et al., *Phys. Lett. B* 712 (2012) 370.
20. S. Dymov et al., *Phys. Lett. B* 712 (2012) 375.
21. R. Bilger et al., *Nucl. Phys. A* 693 (2001) 633.
22. F. Duncan et al., *Phys. Rev. Lett.* 80 (1998) 4390.
23. H. Hahn et al., *Phys. Rev. Lett.* 82 (1999) 2258.
24. H. Hahn et al., *Phys. Rev. C* 53 (1996) 1074.



ANDRO KACHARAVA



COLIN WILKIN